CHEMICAL ENGINEERING TRANSACTIONS
VOL. 127, 2026
A publication of AIDIC
The Italian Association of Chemical Engineering
Online at www.cetjournal.it
Guest Editors: Laura Capelli, Marzio Invernizzi, Selena Sironi

ISBN 979-12-81206-28-1; **ISSN** 2283-9216
DOI: 10.3303/CET26127025

Degradation of Selected Odorants by Hydroxyl Radicals in a Controlled Lab-Scale Reactor: Preliminary Results

Marouane Dhia Eddine Bouguerra, Tomasz Gierczak, Radoslaw Barczak*

Faculty of Chemistry, University of Warsaw, 1 Pasteura Street, 02-093, Warsaw, Poland
rbarczak@chem.uw.edu.pl

Nowadays, the emission of nuisance odorants from Wastewater Treatment Plants (WWTPs) leads to persistent community complaints and localized air quality degradation. Predicting odorants' environmental impact requires a precise characterization of atmospheric lifetimes. This study determined the hydroxyl (•OH) radical reaction kinetics for 1,3,5-trimethylbenzene (TMB), Dimethyl trisulfide (DMTS), and 2-Isopropyl-3-methoxypyrazine (IPMP). Experiments were conducted in a laboratory-scale photochemical reactor, temperature-controlled at 298K via water bath circulation. •OH, were generated in situ through the photolysis of synthesized methyl nitrite (CH_3ONO) within a 305-396 nm window. Using the relative rate method with toluene (TOL) as the reference compound ($k_{ref} = 5.63x10^{-12}$ cm^3 $molecule^{-1}$ s^{-1}), we derived bimolecular reaction rate constants of ($k` = 6.97x10^{-12}$) for TMB, ($k` = 6.39x10^{-12}$) for DMTS, and ($k` = 3.78x10^{-12}$) for IPMP (units: cm^3 $molecule^{-1}$ s^{-1}). Under a standard atmospheric concentration of [•OH] = $1x10^6$ molecules/cm^3, the calculated atmospheric half-lives ($T_{1/2}$) were 27.1 hours (TMB), 30.1 hours (DMTS), and 50.9 hours (IPMP). These results indicate that IPMP exhibits the longest atmospheric lifetime among the studied compounds. The reported kinetic parameters contribute to a more accurate assessment of their atmospheric persistence. Overall, the determined kinetic parameters provide a quantitative basis for assessing the atmospheric degradation rates and persistence of the investigated odorants.

1. Introduction

The nuisance caused by unpleasant odours is a significant concern from both a societal and industrial standpoint (Chaignaud et al., 2014). Nuisance due to odour generation by such as; wastewater treatment plants (WWTPs), landfills, and animal production operations, among others, is one of the major sources of complaints of people living near these facilities (Cao et al., 2023; Czarnota et al., 2023). It has also triggered increased emphasis on controlling the impact of atmospheric pollutants on neighbouring areas (Rincón et al., 2019). Undesirable odours can elicit a range of emotional and adverse responses in individuals, spanning from irritation to documented health effects, ultimately resulting in a diminished quality of life (Blanes-Vidal, 2015). The odours from WWTPs emissions form an intricate mixture containing a diverse range of odorants derived from various chemical groups, including sulphur and nitrogen compounds, aldehydes, acids, alcohols, aromatics, ketones, terpenes, indole, and skatole (Byliński et al., 2019). Only certain malodorous compounds are detected in significant concentrations. The atmosphere can oxidize many pollutants, including odorous species, mainly through the hydroxyl radical (•OH) during the day. Other reactive species, such as nitrate radicals (NO_3), ozone (O_3), chlorine or bromine atoms (Cl or Br), and organic peroxyl radicals (RO_2), also take part in this process (Chapleski et al., 2016). Hydroxyl radicals (•OH) are very important in different parts of the atmosphere (Avallone, 2003). In the troposphere, they are considered the main oxidizing agents for both natural and human-made organic compounds, and they contribute to ozone formation. Hydroxyl radicals are extremely reactive and can easily attack many types of organic compounds. Their strong oxidative ability is related to their high oxidation potential at around 2.8 V (Munter, 2001). In addition, because they are non-selective, they can react with a wide range of organic molecules such as acids, alcohols, aldehydes, aromatic compounds, amines, ethers, and ketones (Huang et al., 1993). However, due to their very short lifetime, hydroxyl radicals must be produced directly in the atmosphere (in situ), mainly through the photolysis of ozone and the reaction of excited oxygen atoms with

Paper Received: 9 March 2026; Revised: 13 May 2026; Accepted: 24 June 2026
Please cite this article as: Bouguerra M.D.E., Gierczak T., Barczak R., 2026, Degradation of Selected Odorants by Hydroxyl Radicals in a Controlled Lab-Scale Reactor: Preliminary Results, Chemical Engineering Transactions, 127, 145-150 DOI:10.3303/CET26127025

water vapor (H_2O), or from the photolysis of nitrous acid (HONO) and hydrogen peroxide (H_2O_2) (Price et al., 2025). In the troposphere, •OH is mainly formed when ozone is broken down by sunlight (photolysis at wavelengths below 282 nm). This process produces oxygen atoms, which then react with water vapor to generate hydroxyl radicals (Avallone, 2003). As a result, •OH is mainly present during the daytime, when sunlight is available.

There is still a lack of knowledge about the reaction kinetics of some odorant compounds with atmospheric oxidants, e.g. •OH, so, limited information about the degradation pace of these odorants. This study focuses on the degradation kinetics of three odorants: 1,3,5-trimethylbenzene (TMB), Dimethyl Trisulfide (DMTS), and 2-Isopropyl-3-methoxypyrazine (IPMP). These compounds are considered important because they are commonly found in emissions from WWTPs, where they contribute significantly to local odour nuisance. To measure their reaction rates with •OH, experiments were carried out using the relative rate method. Since the study was conducted in a controlled lab-scale reactor system specifically designed for •OH generation, the experiments were limited to this single oxidant, as the use of additional atmospheric oxidants such as ozone or nitrate is technically challenging in the current setup. Moreover, the identification of specific degradation products and the elucidation of reaction pathways were beyond the scope of this study, which is primarily focused on determining kinetic parameters.

2. Materials and methods

2.1 Chemicals and reagents

All chemicals and reagents used in this study were of analytical purity and were used without further purification. Sodium hydroxide (Ascarite) and 1,3,5-trimethylbenzene (TMB, ≥98%) were purchased from Thermo Fisher Scientific (USA). 2-Isopropyl-3-methoxypyrazine (IPMP, 99%, food grade) and dimethyl trisulfide (DMTS, ≥98%, food grade) were obtained from Sigma-Aldrich (Germany). Sodium nitrite and anhydrous calcium chloride were supplied by Firma Chempur (Poland). Sulfuric acid (≥95%) was purchased from POCH (Poland). Toluene (GC/MS grade) was obtained from Supelco (Germany). Methanol (LC/MS grade) was purchased from Merck (Germany).

2.2 Methyl Nitrite Synthesis

The methyl nitrite (CH_3ONO) was synthesized in situ, as Atkinson et al. (1981). The dropwise addition of 50% sulfuric acid (H_2SO_4) to methanol (CH_3OH) saturated with sodium nitrite ($NaNO_2$) was carried out at −10 °C under continuous stirring. The generated CH_3ONO was swept from the reaction vessel by a stream of dry, ultra-high purity nitrogen. The gas stream was first passed through a trap containing saturated sodium hydroxide (NaOH) to remove acidic impurities, then dried by passage through a trap filled with anhydrous calcium chloride ($CaCl_2$). Finally, the CH_3ONO was collected in a trap cooled to 196 K using a dry ice/acetone bath. Figure 1 shows the reaction setup.

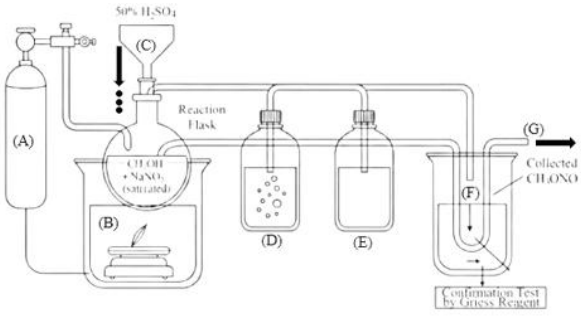

Figure 1: Methyl Nitrite Synthesis setup: (A) Pure nitrogen cylinder, (B) Ice bath, (C) dropping funnel, (D) Trap 1 (containing saturated NaOH), (E) trap 2 (containing anhydrous $CaCl_2$), (F) collecting trap, (G) Nitrogen gas out.

2.3 Experimental Setup and Mechanism of •OH Generation

The experiments were performed in a controlled laboratory-scale photochemical reactor. The temperature was maintained constant at 298 K using a water bath circulation system (Thermo Scientific SC100-25A). •OH, were produced in situ through the photolysis of previously synthesized CH_3ONO. The process was initiated under UV irradiation using a short-arc lamp (Osram XBO 150W/1) equipped with a dichroic bandpass filter (Knight Optical,

50 × 50 mm, transmission range 305-396 nm) to control and monitor the UV irradiation wavelength. Before each experiment, the photolysis reactor was carefully prepared to ensure a clean and stable internal environment. The reactor was first filled with pure air and evacuated three times to remove any remaining impurities. During this step, the temperature was kept constant at 298 K using a circulating water bath. After cleaning, the tightness of the reactor was checked by confirming that a pressure of 50 Torr could be reached. The reactor was then filled with pure air up to 760 Torr (1 atm) before introducing any reactants. Next, to suppress O_3 formation, NO is added to the reaction mixture, which typically consists of approximately 10 ppm of CH_3ONO, 5 ppm of NO, and about 1 ppm each of the target odorant and the reference organic compound. The circulation pump was switched on, and the mixture was left to homogenize for 10 minutes to ensure uniform distribution of all compounds. Finally, the UV lamp was turned on, and the measurements started immediately. The reaction mixture was sampled and injected into the gas chromatography (GC) combined with flame ionization detection (FID) every 10 minutes for a total duration of one hour to monitor the odorant degradation rate under continuous generation of •OH. A total of five replicates were performed.

Upon photolysis of CH_3ONO at known concentrations in pure air, the following reaction sequence occurs (R1-R3). In the presence of added odorants, the generated •OH subsequently reacts with these organic compounds (R4). Figure 2 shows the laboratory-scale photochemical reactor.

$$CH_3ONO + h\nu \rightarrow CH_3O\bullet + NO \quad \text{(R1)}$$

$$CH_3O + O_2 \rightarrow HCHO + HO_2\bullet \quad \text{(R2)}$$

$$HO_2 + NO \rightarrow \bullet OH + NO_2 \quad \text{(R3)}$$

$$\bullet OH + odor \rightarrow products \quad \text{(R4)}$$

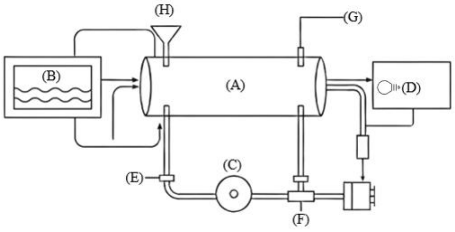

Figure 2: Constructed Lab-scale reactor: (A) Photolysis chamber, (B) Circulation water bath, (C) Circulation pump, (D) Light source, (E) Pure air valve, (F) Sucking pump, (G) Pressure measuring device, (H) Injection port.

2.4 Gas Chromatography Measurements

Gas chromatography measurements were performed using a Shimadzu GC-17A equipped with a Flame Ionization Detector (FID) and a Supelco SPB-1 capillary column (60 m × 0.32 mm × 1.0 µm). A 500 µL gas-tight syringe by Hamilton was used for manual injections. The injector and detector temperatures were maintained at 220 °C and 250 °C, respectively, while the oven temperature was held constant at 175 °C under isothermal conditions. Headspace samples were withdrawn from the injection port of the laboratory-scale reactor (Figure 2) every 10 minutes and injected manually into the GC system. The degradation of TMB, DMTS, and IPMP was monitored by tracking the decrease in their peak areas, with toluene used as the reference compound.

2.5 Estimating Atmospheric Lifetimes

The lifetime is calculated using pseudo-first-order kinetics, where it is assumed that the oxidant concentration stays nearly constant over the reaction time (a total of 70 minutes, including 10 minutes in the dark and 60 minutes under UV irradiation).

The general equation used to determine the lifetime of an odorant compound [B] with respect to a given oxidant [A] is shown in Eq. 2 (Wang et al., 2022).

$$ln\left(\frac{[B]_0[A]_t}{[B]_t[A]_0}\right) = kt([A]_0 - [B]_0) \quad (1)$$

Substituting this into the equation, we get:

$$T\frac{1}{2} = \frac{1}{k([A]_0 - [B]_0)} \ln\left(2\frac{[A]_0}{[A]_t}\right) \quad (2)$$

Where are: $[A]_0$: Initial concentration of an oxidant at time; t=0; $[B]_0$: Initial concentration of an odorant at time, t=0; $[A]_t$: Concentration of an oxidant later; $[B]_t$: Concentration of an odorant later; k: Rate coefficient for the reaction between A and B; $T_{1/2}$: Half-life of B
Introducing the relative rate method, we get:

$$K_B = R\ K_{ref} \quad (3)$$

$$K` = K_B\ [OH]_{standard} \quad (4)$$

Where are: K_B: Rate coefficient for odorant; K_{ref}: Rate coefficient for reference (from literature); R: Is the slope extracted from plotting $Ln(odorant_0/odorant_t)$ Vs $Ln(ref_0/ref_t)$; K`: Pseudo-First-Order Reaction Rate
Substituting this into the equation, we get:

$$T\frac{1}{2} = \frac{\ln(2)}{K`} \quad (5)$$

3. Results and discussion

The relative rate method is a commonly applied approach in atmospheric chemistry for determining the reaction rate constant of a target compound by comparing its degradation rate with that of a reference compound whose rate constant toward the same oxidant (•OH) is already known (Xin et al., 2024). This method was chosen because it minimizes the influence of experimental fluctuations, such as variations in injection volume or pressure. Rather than depending on the absolute concentration of •OH, which may vary during the experiment, the technique is based on monitoring the relative decay of both the target and reference compounds as a function of time. The method assumes that both compounds react only with the same oxidant and are subjected to identical experimental conditions. Figure 3 shows the time-dependent degradation profiles of MST, DMTS, and IPMP, along with the corresponding relative rate plots obtained. Based on the equations used to estimate atmospheric lifetimes, the half-lives of the investigated odorants were calculated accordingly. Table 1 presents a comprehensive summary of the kinetic and statistical parameters and results obtained in this study. It combines the experimentally determined relative rate constants and their corresponding R^2 values derived from linear regression constrained to pass through the origin with the literature rate constant of the reference compound, toluene, equal to $5.63x10^{-12}$ cm^3 $molecule^{-1}$ s^{-1} as (Bohn, 2001). Using an average atmospheric •OH concentration at $1x10^6$ molecules/cm^3 as studied by Atkinson (2000), the relative rate data were then used to determine the rate constants (k) and to estimate the atmospheric half-lives ($T_1/_2$) of each odorant. The calculated atmospheric half-lives ($T_1/_2$) were 27.6 hours for TMB, 30.1 hours for DMTS, and 50.9 hours for IPMP, highlighting differences in their reactivity toward •OH. These values were calculated assuming a fixed •OH concentration similar to a typical daytime average. In different environments, where the •OH concentration is higher or lower than this average, the half-lives will change. In particular, the half-life of each odorant decreases when •OH is more abundant (faster reactions) and increases when •OH is less abundant (slower reactions). In addition, the half-life is also affected by the initial concentration of the odorant itself, although the relative trends in reactivity (TMB most reactive, IPMP most persistent) remain consistent under similar reaction conditions.

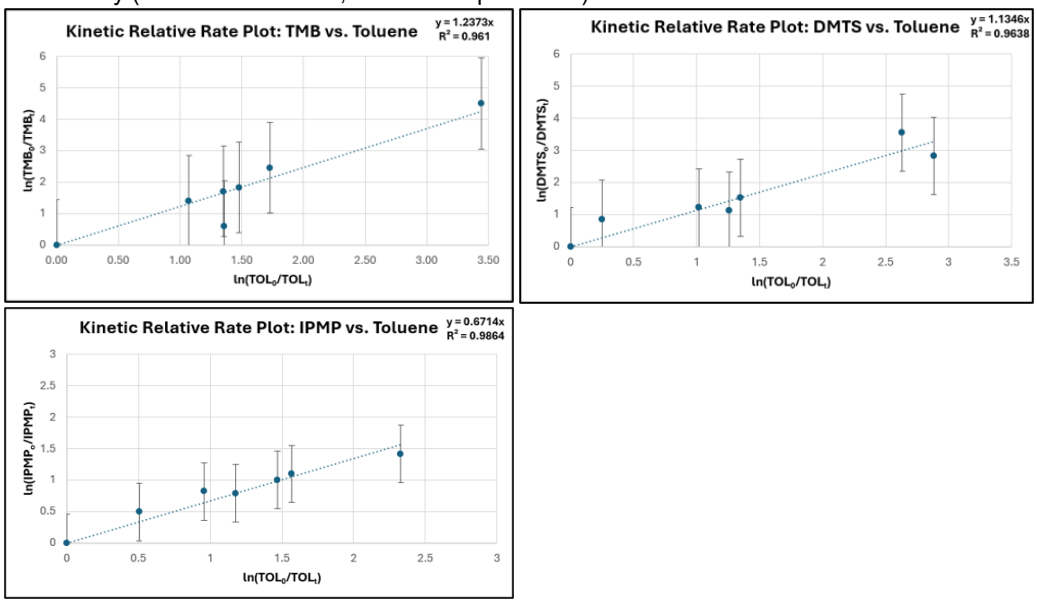

Figure 3: The relative rate plots of TMB, DMTS, and IPMP obtained using toluene as the reference compound.

Table 1: The kinetics and statistical parameters were derived from the relative rate method.

Parameters	TMB	DMTS	IPMP
Relative Rate (R±SE)	1.24±0.07	1.14±0.09	0.67±0.03
Reliability (R^2)	0.961	0.9638	0.9864
K (Rate Constant) (cm^3/molecule x s)	6.97 x 10^{-12}	6.39 x 10^{-12}	3.78 x 10^{-12}

4. Conclusion

In this work, •OH radicals were successfully generated via CH_3ONO photolysis, and the degradation of key odorants (TMB, DMTS, and IPMP) was systematically monitored within the reactor. By applying the relative rate method, reaction rate constants and atmospheric half-lives were calculated, which are both kinetic parameters that describe the atmospheric fate of these compounds.

Based on the derived relative rates, IPMP was identified as the most persistent compound, whereas TMB exhibited the highest reactivity, indicating a shorter atmospheric half-life and a faster decline in concentration due to its reaction with hydroxyl radicals. These results suggest that IPMP may remain in the atmosphere longer than TMB and DMTS under similar •OH exposure conditions, which could extend its potential for odor perception at greater distances from the emission source.

Although some R^2 values were slightly lower for MST and DMTS, the overall dataset still provides a meaningful indication of their degradation behaviour in the reactor and supports the extrapolation to atmospheric kinetic behaviour for odorants. Hence, this work should be regarded as a preliminary investigation. Future research will explore a broader range of temperatures and environmental conditions to better represent atmospheric variability.

Acknowledgment

This work was supported by an OPUS-21 no UMO-2021/41/B/ST8/03440 from National Science Centre, Poland. The authors would like to express their sincere gratitude to Dr hab. Bartłomiej Witkowski for his valuable technical support and assistance during the laboratory experiments.

References

Atkinson, R. (2000). Atmospheric chemistry of VOCs and NOx. Atmospheric Environment, 34(12), 2063-2101. https://doi.org/https://doi.org/10.1016/S1352-2310(99)00460-4

Atkinson, R., Carter, W. P. L., Winer, A. M., & Pitts, J. N. (1981). An Experimental Protocol for the Determination of OH Radical Rate Constants with Organics Using Methyl Nitrite Photolysis as an OH Radical Source. Journal of the Air Pollution Control Association, 31(10), 1090-1092. https://doi.org/10.1080/00022470.1981.10465331

Avallone, L. M. (2003). OBSERVATIONS FOR CHEMISTRY (IN SITU) | Resonance Fluorescence. In J. R. Holton (Ed.), Encyclopedia of Atmospheric Sciences (pp. 1484-1490). Academic Press. https://doi.org/https://doi.org/10.1016/B0-12-227090-8/00260-8

Blanes-Vidal, V. (2015). Air pollution from biodegradable wastes and non-specific health symptoms among residents: Direct or annoyance-mediated associations? Chemosphere, 120, 371-377. https://www.sciencedirect.com/science/article/pii/S0045653514009679

Bohn, B. (2001). Formation of Peroxy Radicals from OH−Toluene Adducts and O2. The Journal of Physical Chemistry A, 105(25), 6092-6101. https://doi.org/10.1021/jp0033972

Byliński, H., Barczak, R. J., Gębicki, J., & Namieśnik, J. (2019). Monitoring of odors emitted from stabilized dewatered sludge subjected to aging using proton transfer reaction–mass spectrometry [journal article]. Environmental Science and Pollution Research, 26(6), 5500-5513. https://doi.org/http://doi.org/10.1007/s11356-018-4041-4

Cao, T., Zheng, Y., & Dong, H. (2023). Control of odor emissions from livestock farms: A review. Environ Res, 225, 115545. https://doi.org/10.1016/j.envres.2023.115545

Chaignaud, M., Cariou, S., Poette, J., Fages, M., Despres, J. F., & Fanlo, J. L. (2014). A new method to evaluate odour annoyance potential. Chemical Engineering Transactions, 40(13-18).

Chapleski, R. C., Zhang, Y., Troya, D., & Morris, J. R. (2016). Heterogeneous chemistry and reaction dynamics of the atmospheric oxidants, O3, NO3, and OH, on organic surfaces [10.1039/C5CS00375J]. Chemical Society Reviews, 45(13), 3731-3746. https://doi.org/10.1039/C5CS00375J

Czarnota, J., Masłoń, A., & Pajura, R. (2023). Wastewater Treatment Plants as a Source of Malodorous Substances Hazardous to Health, Including a Case Study from Poland. Int J Environ Res Public Health, 20(7). https://doi.org/10.3390/ijerph20075379

Huang, C. P., Dong, C., & Tang, Z. (1993). Advanced chemical oxidation: Its present role and potential future in hazardous waste treatment. Waste Management, 13(5), 361-377. https://doi.org/https://doi.org/10.1016/0956-053X(93)90070-D

Munter, R. (2001). ADVANCED OXIDATION PROCESSES – CURRENT STATUS AND PROSPECTS. Proceedings of the Estonian Academy of Sciences. Chemistry.

Price, P., Bottorff, B., Jenkins, J., Brune, W. H., & Stevens, P. S. (2025). Re-assessing hydroxyl radical chemistry in the atmosphere: Instrument interferences may explain previous measurement discrepancies. Communications Earth & Environment, 6(1), 325. https://doi.org/10.1038/s43247-025-02308-y

Rincón, C. A., De Guardia, A., Couvert, A., Le Roux, S., Soutrel, I., Daumoin, M., & Benoist, J. C. (2019). Chemical and odor characterization of gas emissions released during composting of solid wastes and digestates. Journal of Environmental Management, 233, 39-53. https://doi.org/https://doi.org/10.1016/j.jenvman.2018.12.009

Wang, W., Yuan, B., Peng, Y., Su, H., Cheng, Y., Yang, S., Wu, C., Qi, J., Bao, F., Huangfu, Y., Wang, C., Ye, C., Wang, Z., Wang, B., Wang, X., Song, W., Hu, W., Cheng, P., Zhu, M.,…Shao, M. (2022). Direct observations indicate photodegradable oxygenated volatile organic compounds (OVOCs) as larger contributors to radicals and ozone production in the atmosphere. Atmos. Chem. Phys., 22(6), 4117-4128. https://doi.org/10.5194/acp-22-4117-2022

Xin, Y., Liu, C., Lun, X., Xie, S., Liu, J., & Mu, Y. (2024). Rate coefficients for the reactions of OH radicals with C3–C11 alkanes determined by the relative-rate technique. Atmos. Chem. Phys., 24(19), 11409-11429. https://doi.org/10.5194/acp-24-11409-2024